

**Iodine-Doped ZnO Nanocrystalline Aggregates  
for Improved Dye-Sensitized Solar Cells**Yan-Zhen Zheng,<sup>†,‡</sup> Xia Tao,<sup>\*,†</sup> Qian Hou,<sup>†</sup>  
Dong-Ting Wang,<sup>†</sup> Wei-Lie Zhou,<sup>§</sup> and  
Jian-Feng Chen<sup>\*,‡</sup>

<sup>†</sup>Key Laboratory for Nanomaterials of the Ministry of Education, Beijing University of Chemical Technology, Beijing 100029, China, <sup>‡</sup>Research Center of the Ministry of Education for High Gravity Engineering & Technology, Beijing University of Chemical Technology, Beijing 100029, China, and <sup>§</sup>Advanced Materials Research Institute University of New Orleans New Orleans, Louisiana 70148, United States

Received May 31, 2010

Revised Manuscript Received November 9, 2010

Dye-sensitized solar cells (DSSCs) have demonstrated promise for solar-energy conversion to electricity because of their low fabrication cost, easy manufacture process, and relatively high efficiency.<sup>1</sup> The primary photovoltaic (PV) material for DSSCs today is TiO<sub>2</sub>, for which conversion efficiencies greater than 11% have been successfully achieved.<sup>2</sup> In contrast, other metal oxide semiconductors, such as zinc and tin oxides, have received less attention, though these materials possess comparable band gap widths and photoelectrochemical properties to TiO<sub>2</sub>.<sup>3–7</sup> ZnO has higher electron mobility ( $\sim 205\text{--}1000\text{ cm}^2\text{ V}^{-1}\text{ s}^{-1}$ ) than TiO<sub>2</sub> ( $\sim 0.1\text{--}4\text{ cm}^2\text{ V}^{-1}\text{ s}^{-1}$ ), enabling faster diffusion transport of photoinjected electrons when employed as the electrode in DSSCs.<sup>8</sup> Moreover, ZnO can be easily processed into various nanostructures, such as nanoparticles,<sup>9</sup> nanowires,<sup>4,5</sup> nanotubes,<sup>3</sup> and tetrapods,<sup>10</sup> providing numerous options for optimizing the electrode morphology so as to improve the charge collection. However, the conversion efficiency of ZnO-based DSSCs reported so far still remains lower than those fabricated from TiO<sub>2</sub>, leaving plenty of room to improve the efficiency through structural and morphology modification of the electrode.

\*Corresponding author. E-mail: taoxia@yahoo.com (X.T.), chenjf@mail.buct.edu.cn (J.-F.C.).

- (1) Xu, H.; Tao, X.; Wang, D.-T.; Zheng, Y.-Z.; Chen, J.-F. *Electrochim. Acta* **2010**, *55*, 2280.
- (2) Grätzel, M. *Inorg. Chem.* **2005**, *44*, 6841.
- (3) Guo, M.; Diao, P.; Cai, S. *Chin. Chem. Lett.* **2004**, *15*, 1113.
- (4) Guo, M.; Diao, P.; Wang, X.; Cai, S. *J. Solid State Chem.* **2005**, *178*, 3210.
- (5) Gao, Y.; Nagai, M.; Chang, T.-C.; Shyue, J.-J. *Cryst. Growth Des.* **2007**, *7*, 2467.
- (6) Wang, K.; Chen, J.; Zhou, W.; Zhang, Y.; Yan, Y.; Pern, J.; Mascarenhas, A. *Adv. Mater.* **2008**, *20*, 3248.
- (7) Qian, J.; Liu, P.; Xiao, Y.; Jiang, Y.; Cao, Y.; Ai, X.; Yang, H. *Adv. Mater.* **2009**, *21*, 3663.
- (8) Zhang, Q.; Dandeneau, C. S.; Zhou, X.; Cao, G. *Adv. Mater.* **2009**, *21*, 4087.
- (9) Rensmo, H.; Keis, K.; Lindstrom, H.; Sodergren, S.; Solbrand, A.; Hagfeldt, A.; Lindquist, S. E.; Wang, L.; Muhammed, M. *J. Phys. Chem. B* **1997**, *101*, 2598.
- (10) Yang, Z.; Xu, T.; Ito, Y.; Welp, U.; Kwok, W. K. *J. Phys. Chem. C* **2009**, *113*, 20521.

One way to enhance the efficiency of ZnO-based cells is to construct one-dimensional nanostructures that produce more direct electron transport path so as to increase electron diffusion length and reduce the charge recombination rate.<sup>3–6</sup> To this end, aligned nanowire/nanorod arrays,<sup>4</sup> individual nanowires,<sup>5</sup> and inorganic core/shell nanowire architectures<sup>11</sup> have been fabricated as the anode, with which an efficiency of 2.4% was achieved in the most successful case.<sup>4,11</sup> Another approach is to improve the light-harvesting capability of the film by taking the optical enhancement effects, i.e., additional admixing of submicrometer-sized ZnO particles as the light-scattering centers and/or direct introduction of a light-scattering layer in the photoelectrode film.<sup>12–14</sup> Particularly, ZnO aggregates composed of nanosized crystallites can be used as efficient light scatters, offering relatively large specific surface area framework, and removing the adverse effect caused by the lowered adsorption of dye-molecules in the film. For the case employing hierarchical structure of  $\sim 300\text{ nm}$  ZnO colloids, such approach can increase the conversion efficiency up to 3.5%.<sup>14</sup> Extending the spectral response to the visible region represents another way to enhance the light-harvesting capability of the electrode. Typically, visible response of ZnO nanomaterials can be realized by doping nonmetal elements such as N, S, and C as previously reported for photocatalytic degradation of pollutants and photoelectrochemical water splitting, where ZnO was used as the photocatalysts.<sup>15,16</sup> The non-metal-doping not only narrows the band gap so as to be responsible for visible light, but also inhibits the recombination of photogenerated electrons and holes.<sup>16</sup> Combination of these two features will likely produce higher efficiency for ZnO-based DSSCs. Nevertheless, to the best of our knowledge, there has been no report on the DSSCs that employ non-metal-doped ZnO as the photoelectrode.

In this communication, we report on a hierarchically structured PV nanomaterial based on iodine-doped ZnO nanocrystalline aggregates (denoted as ZnO:I) exhibiting large internal surface area as well as strong light-scattering property, which can be used as effective photoanode in DSSCs. Iodine has proven to be a promising dopant for n-type materials to extend the visible response.

- (11) Hamann, T. W.; Martinson, A. B. F.; Elam, J. W.; Pellin, M. J.; Hupp, J. T. *Adv. Mater.* **2008**, *20*, 1560.
- (12) Zheng, Y.-Z.; Tao, X.; Wang, L.-X.; Xu, H.; Hou, Q.; Zhou, W.-L.; Chen, J.-F. *Chem. Mater.* **2010**, *22*, 928.
- (13) Zhang, Q.; Chou, T. P.; Russo, B.; Jenekhe, S. A.; Cao, G. *Adv. Funct. Mater.* **2008**, *18*, 1654.
- (14) Chou, T. P.; Zhang, Q.; Fryxell, G. E.; Cao, G. *Adv. Mater.* **2007**, *19*, 2588.
- (15) Yang, X.; Wolcott, A.; Wang, G.; Sobo, A.; Fitzmorris, R. C.; Qian, F.; Zhang, J. Z.; Li, Y. *Nano Lett.* **2009**, *9*, 2331.
- (16) Chen, L.-C.; Tu, Y.-J.; Wang, Y.-S.; Kan, R.-S.; Huang, C.-M. *J. Photochem. Photobiol. A: Chem.* **2008**, *199*, 170.

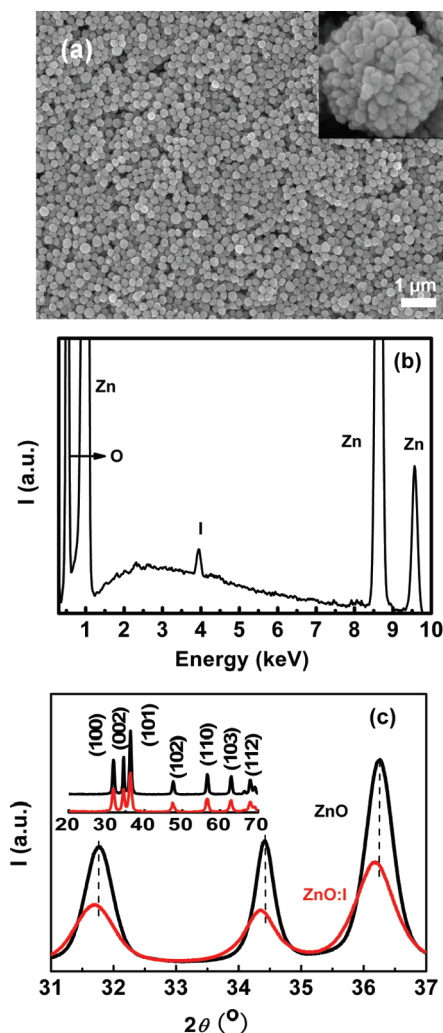


**Figure 1.** (a) FESEM image of as-prepared ZnO:I. Inset showing a magnified FESEM image of single aggregate. (b) EDS spectrum of ZnO:I sample. Strong Zn peaks, as well as weak I atomic peaks at around 3.94 keV, were detected in the EDS spectrum. (c) The fine-scanned (100), (002), and (101) peaks of ZnO and ZnO:I, showing the peak broadening and shifting due to the doping. The inset shows a full-range XRD patterns, indexing as wurtzite hexagonal ZnO.

The doped iodine can often act as trapping site for the electrons, thus preventing the unwanted charge recombination.<sup>17–19</sup> When fabricated as the photoanode in DSSCs, the multifunctional ZnO:I films as-prepared produced an efficiency of 4.5%, almost double that of undoped ZnO aggregates (2.3%). This finding adds fundamental insight into the ZnO-based DSSCs and provides new options for improving the conversion efficiency.

Highly monodispersed and spherically structured ZnO: I nanocrystalline aggregates were synthesized by the solvothermal process from zinc salt and iodic acid in polyol medium along with heating at 160 °C. The experimental details of synthesis are provided in the Supporting Information. For comparison, pristine monodispersed

ZnO nanocrystalline aggregates were fabricated following the similar synthesis procedure. Scanning electron microscopy (SEM) image (Figure 1a) of ZnO:I shows that ~250 nm-sized monodispersed aggregates are nearly spherical in shape and each aggregate consists of random agglomeration of tiny nanocrystalline particles (inset of Figure 1a). Transmission electron microscopy (TEM) image (see Figure S1 in the Supporting Information) reveals that ZnO:I aggregates are well-defined and porous. Energy-dispersive spectroscopy (EDS) measurement demonstrates the existence of iodine in ZnO matrix (Figure 1b). By scanning spherical aggregates of ZnO:I in different areas, the average iodine concentration is estimated to be ~2.2 wt % (see Figure S2 in the Supporting Information), which is in good agreement with the result obtained by a high-resolution X-ray photoelectron spectroscopy (see Figure S3 in the Supporting Information). Additionally, the shift of fine-scanned X-ray diffraction (XRD) peaks has been employed to demonstrate a discernible change in the lattice constants due to doping.<sup>20–22</sup> As can be seen from the Figure 1c, the strong diffractive peaks of ZnO:I with the index of (100), (002) and (101) shift toward lower  $2\theta$  values and the peak width broadens in comparison to the pristine ZnO, suggesting the successful doping of I in ZnO crystal structure. The inset shows the full-range XRD patterns of undoped and doped ZnO, indexing as wurtzite hexagonal ZnO. The crystallite sizes are estimated around 22 and 16 nm for undoped and doped ZnO nanoparticles, respectively. Further evidence (see Figures S3 and S4 in the Supporting Information) and discussion for the doping of I into the ZnO lattice are given in the Supporting Information.

The ZnO:I film of approximately 8  $\mu\text{m}$  in thickness (see Figure S5 in the Supporting Information) was formed using a drop-cast method onto a fluorine-doped tin oxide (FTO) coated glass substrate and subsequently followed by calcinations at 350 °C for 60 min in air. For comparison, undoped ZnO film with thickness of ~8  $\mu\text{m}$  identical to that of the ZnO:I film was also prepared, and it was found that the two films maintained analogous structure and morphology (see Figure S6 in the Supporting Information). To study the PV performance of undoped and doped-ZnO based DSSCs, undoped ZnO as well as ZnO:I films were adopted to form photoanodes of DSSCs, and their current–voltage characteristics were measured under the AM1.5 simulated sunlight with a power density of 100  $\text{mW}/\text{cm}^2$  (Figure 2). For the ZnO-based cell, the  $J_{\text{sc}}$  of 9.0  $\text{mA}/\text{cm}^2$ ,  $V_{\text{oc}}$  of 612 mV and  $\eta$  of 2.3% were achieved. The efficiency thus obtained is within the range (1.5%–2.7%) that is typically achieved for the cells based on 160–350 nm-sized monodispersed spherical ZnO aggregates without doping.<sup>13</sup> After doping with iodine, the  $J_{\text{sc}}$  and  $\eta$  were significantly increased, reaching a maximum of up to 14.0  $\text{mA}/\text{cm}^2$  and 4.5%,

(17) Usseglio, S.; Calza, P.; Damin, A.; Minero, C.; Bordiga, S.; Lamberti, C.; Pelizzetti, E.; Zecchina, A. *Chem. Mater.* **2006**, *18*, 3412.  
 (18) Usseglio, S.; Damin, A.; Scarano, D.; Bordiga, S.; Zecchina, A.; Lamberti, C. *J. Am. Chem. Soc.* **2007**, *129*, 2822.  
 (19) Tojo, S.; Tachikawa, T.; Fujitsuka, M.; Majima, T. *J. Phys. Chem. C* **2008**, *112*, 14948.

(20) Alpuche-Aviles, M. A.; Wu, Y. *J. Am. Chem. Soc.* **2009**, *131*, 3216.  
 (21) Cui, J. B.; Soo, Y. C.; Chen, T. P.; Gibson, U. *J. Phys. Chem. C* **2008**, *112*, 4475.  
 (22) Sheini, F. J.; More, M. A.; Jadkar, S. R.; Patil, K. R.; Pillai, V. K.; Joag, D. S. *J. Phys. Chem. C* **2010**, *114*, 3843.

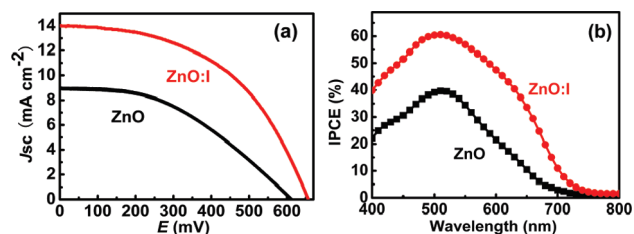


**Figure 2.** (a) Photocurrent–voltage characteristics and (b) IPCE spectra of DSSCs based on ZnO and ZnO:I.

respectively. The highest  $\eta$  of ZnO:I cell corresponds to a 96% increment of undoped ZnO cell. Besides, the adsorbed amount of dye in ZnO or ZnO:I films were determined by measuring the eluted dye concentrations with UV–vis absorption spectroscopy. It was found that almost identical adsorption amount of dye was in the films before ( $5.16 \times 10^{-8} \text{ mol cm}^{-2}$ ) and after iodine doping ( $5.38 \times 10^{-8} \text{ mol cm}^{-2}$ ), which is in good agreement with their analogous BET data ( $51.0$  and  $59.7 \text{ m}^2 \text{ g}^{-1}$  for ZnO and ZnO:I, respectively) as well as film texture framework. Thus, the performance enhancement of ZnO:I cells can be reasonably inferred to be arising from the intrinsic components of the films as well as sunlight harvesting and photon-to-electron transfer process of the cells.

To find out the reasons for a higher photocurrent result for a solar cell based on ZnO:I, we measured incident photon to current conversion efficiency (IPCE) to study the photoactive wavelength regime for the undoped and doped ZnO cells (Figure 2b). Notably, IPCE data of the ZnO:I cell show a red shift, facilitating the utilization of sunlight in the full spectrum range. Such a red shift was also observed in UV–vis absorption spectroscopy measurements (see Figure S4 in the Supporting Information). Besides, IPCE profile of ZnO:I cell is found broadened and strengthened over the entire wavelength region compared with that of undoped ZnO cell. The maxima of IPCE value measured at approximately 510 nm are 42 and 61% for ZnO and ZnO:I cells, respectively.

To gain further insight into electron transport and recombination properties of the ZnO:I cell, we measured electrochemical impedance spectroscopy (EIS) spectra (Figure 3) at an applied bias of  $V_{oc}$  under illumination. In the Nyquist plots (see the inset of Figure 3) a well-defined semicircle in the low-frequency region (100–1 Hz) attributed to electron transfer at the ZnO/dye/electrolyte interface dominates the impedance of the DSSC, and is recognized as the characteristic shape of recombination through the semiconductor.<sup>7</sup> Under  $V_{oc}$  condition, no current passes through the external circuit, and the electrons injected into ZnO or ZnO:I must be recombined by redox electrolyte at the ZnO/dye/electrolyte interface. Electron lifetime ( $\tau_e$ ) in the ZnO-based films can be determined from the maximum frequency of the low-frequency peak ( $f_{max}$ ) value following the equation

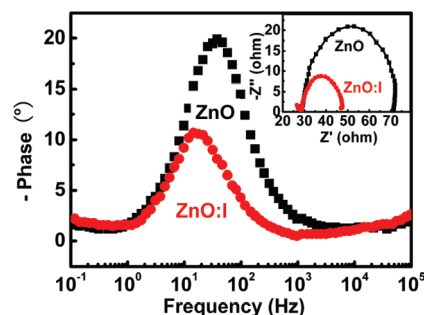


**Figure 3.** Bode phase plots of DSSCs based on ZnO and ZnO:I measured at the  $V_{oc}$  under  $100 \text{ mW cm}^{-2}$  illumination. The inset displays the Nyquist plots of the two cells.

$\tau_e = 1/\omega_{max} = 1/2\pi f_{max}$ .<sup>23–25</sup> Bode phase plots (Figure 3) show that iodine doping in ZnO led to a decrease in the  $f_{max}$  values, and  $\tau_e$  is determined to be 4.7 and 12.3 ms for ZnO and ZnO:I cells, respectively. This means that the electron transfer through a longer distance is unblocked to a larger extent across the ZnO:I/dye/electrolyte interface, leading to more effective capture and collection of electrons. The increased  $\tau_e$  and decreased charge recombination found for the ZnO:I cell could be attributed to the doped iodine, which acts as charge trapping site for the electron–hole separation, hence leading to the enhancement of photon-to-electron conversion efficiency.<sup>8,23–26</sup>

In summary, monodispersed ZnO:I nanocrystalline aggregates synthesized by a facile solvothermal process were used as photoanodes of DSSCs, which exhibited improved cell performance with an efficiency of up to 4.5%. IPCE spectra of ZnO:I cell exhibited a significant enhancement in light harvesting, especially in the visible region. EIS data and analysis results further confirmed that I doping lowered recombination resistance and prolonged electron lifetime of the hierarchically structured ZnO cell, thus diminishing the recombination process. Therefore, ZnO:I may be developed as a promising photoelectrode material for high-efficiency DSSCs. The reported doping system is expandable to other non-metal-doped semiconductors that may be used to enhance the DSSC performance.

**Acknowledgment.** This work was supported financially by NSFC (20776014, 20906004, 20977005, 20821004), special grade of CPSF (201003042), 863 project (2007AA03Z343).

**Supporting Information Available:** Experimental details, SEM and TEM images of ZnO:I, EDS results, XPS spectra, and UV–vis spectra (PDF). This material is available free of charge via the Internet at <http://pubs.acs.org>.

- (23) Lagemaat, J.; Park, N.-G.; Frank, A. J. *J. Phys. Chem. B* **2000**, *104*, 2044.
- (24) Papageorgiou, N.; Maier, W. F.; Grätzel, M. *J. Electrochem. Soc.* **1997**, *144*, 876.
- (25) Wang, H.; He, J.; Boschloo, G.; Lindström, H.; Hagfeldt, A.; Lindquist, S.-E. *J. Phys. Chem. B* **2001**, *105*, 2529.
- (26) Zhao, D.; Chen, C.; Wang, Y.; Ji, H.; Ma, W.; Zang, L.; Zhao, J. *J. Phys. Chem. C* **2008**, *112*, 5993.